

Structural determination of argon trimer

Cite as: AIP Advances 5, 097213 (2015); <https://doi.org/10.1063/1.4932041>

Submitted: 05 August 2015 • Accepted: 17 September 2015 • Published Online: 25 September 2015

Xiguo Xie, Chengyin Wu, Ying Yuan, et al.



View Online



Export Citation



CrossMark

ARTICLES YOU MAY BE INTERESTED IN

[Three-body fragmentation of CO₂ driven by intense laser pulses](#)

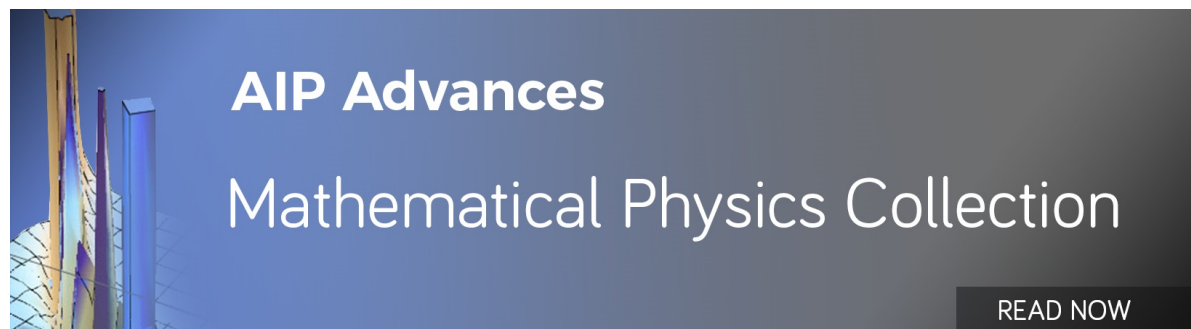
The Journal of Chemical Physics **142**, 124303 (2015); <https://doi.org/10.1063/1.4916045>

[Communication: Determining the structure of the N₂Ar van der Waals complex with laser-based channel-selected Coulomb explosion](#)

The Journal of Chemical Physics **140**, 141101 (2014); <https://doi.org/10.1063/1.4871205>

[Calculation of argon trimer rovibrational spectrum](#)

The Journal of Chemical Physics **126**, 174305 (2007); <https://doi.org/10.1063/1.2721564>



AIP Advances
Mathematical Physics Collection

READ NOW

Structural determination of argon trimer

Xiguo Xie,¹ Chengyin Wu,^{1,2,a} Ying Yuan,³ Xin-Zheng Li,^{2,3,a} Cong Wu,¹
Peng Wang,¹ Yongkai Deng,¹ Yunquan Liu,^{1,2} and Qihuang Gong^{1,2}

¹State Key Laboratory for Mesoscopic Physics, Department of Physics, Peking University,
Beijing 100871, P. R. China

²Collaborative Innovation Center of Quantum Matter, Beijing 100871, P. R. China

³School of Physics, Peking University, Beijing 100871, P. R. China

(Received 5 August 2015; accepted 17 September 2015; published online 25 September 2015)

Rare gas clusters are model systems to investigate structural properties at finite size. However, their structures are difficult to be determined with available experimental techniques because of the strong coupling between the vibration and the rotation. Here we experimentally investigated multiple ionization and fragmentation dynamics of argon trimer by ultrashort intense laser fields and reconstructed their structures with Coulomb explosion technique. The measured structure distribution was compared with our finite-temperature *ab initio* calculations and the discrepancy was discussed. The present study provides a guidance for the development of theoretical methods for exploring the geometric structure of rare gas clusters. © 2015 Author(s). All article content, except where otherwise noted, is licensed under a Creative Commons Attribution 3.0 Unported License. [<http://dx.doi.org/10.1063/1.4932041>]

I. INTRODUCTION

Rare gas clusters are made of rare gas atoms through van der Waals forces and are the most weakly bound of all clusters. Theoretical explorations have been extensively carried out to predict their structures, dynamics and thermodynamics.^{1,2} Due to the knowledge of accurate pair-wise interaction potentials, they serve as excellent model systems to investigate the structural properties of clusters at finite size.³⁻⁵ It has been predicted that their unique structures can be changed by adding a single atom or electron. Among them helium cluster structures have been attracted much attention because of the dominant role of quantum effects. The results demonstrated that ⁴He clusters are bound at all sizes. In the case of He₂, the binding energy is only 95 neV and the mean value of the internuclear distance is 52 Å.⁶⁻¹⁰ He₃ is more tightly bound than He₂. However, various preferred shapes of He₃ have been predicted, from the quasi-linear to the equilateral triangle.¹¹⁻¹⁵ In the case of Ar₃, the geometric structure is predicted to be equilateral triangle. Some other structure-distinct isomers, such as T-shaped structure and linear structure, appear when the temperature is beyond 20 K.^{16,17} In contrast, the structure of Ar₃⁺ is predicted to be linear up to about 300 K.¹⁸ Bressanini and Morosi compared those theoretical predictions and found a number of disagreements among them.¹⁵ Unfortunately, the structure of rare gas clusters remains difficult to be determined with available experimental techniques, such as spectroscopic method and diffraction method, because of the floppy structure. Novel experimental techniques are required to determine the structure of rare gas clusters. These experimentally measured structural parameters are important for testing theoretical predictions and guiding the development of theoretical methods.

It has been demonstrated that laser-induced Coulomb explosion technique can image molecular structures,¹⁹⁻²⁶ in which molecules are multiply ionized by short intense laser pulses. Due to the Coulomb repulsive forces, multiply charged molecular ions are quickly fragmented through the process of so-called Coulomb explosion and their structures can be deduced from momentum vectors of correlated atomic ions produced in the explosion process. However, there are still some

^aEmail: cywu@pku.edu.cn; xzli@pku.edu.cn

challenges for imaging molecular structures using laser-based Coulomb explosion technique due to the complicated laser-molecule interaction.²⁷ The first challenge is to correctly identify the Coulomb explosion channel. It is known that many-body fragmentation can occur through a sequential process (a stepwise breakup process by emitting fragmental ions one after the other with the existence of an intermediate) or Coulomb explosion process (a concerted breakup process with all bonds break simultaneously by their Coulomb repulsion forces).^{22,28} Proficient experimental technique and data processing skill are required to separate the experimental data of Coulomb explosion and sequential fragmentation. The second challenge is to ensure the molecular structure unchanged during the multiple ionization induced by intense laser fields. Structural deformation and bond length stretching often occur during the ionization process depending on the laser parameters. Therefore, when imaging molecular structures using Coulomb explosion technique, laser pulses with suitable parameters are required to ensure that the molecular structure is kept unchanged during the process of multiple ionization and all molecules have the same probability to be ionized in the laser focus regardless of their structures.²⁹ Only these conditions are met, the reconstructed structural parameters for molecular ions can really represent the structure of the neutral molecules before the laser irradiation. The third challenge is to convert the momentum vectors of correlated atomic ions into the structural parameters of molecular ions. Coulomb potential approximation is always applied in the reconstruction of molecular structure due to the lack of the *ab initio* many-body fragmentation potential surface. However, the approximation is not always accurate to describe the Coulomb explosion process, especially when the internuclear distance is not large.^{22,30}

Laser-based Coulomb explosion is a feasible method to image the structure of rare gas clusters because they have large equilibrium internuclear distances^{17,18} and Coulomb potential is accurate enough to describe the explosion dynamics. Ulrich *et al.* studied the structure of the neon and argon dimer, trimer and tetramer using the Coulomb explosion imaging.²³ The results show that the reconstructed structural distribution agrees with the theoretical calculation for neon trimer. However, the reconstructed angular distribution is broader than that calculated by the theory for argon trimer. The discrepancy between the reconstructed structure and the theoretical prediction has attracted significant attention. One possible explanation is that the molecular structure is changed during the multiple ionization. Thus the reconstructed structure of Ar_3^{3+} cannot represent the structure of Ar_3 before laser irradiation. In this article, we systematically investigated multiple ionization and Coulomb explosion dynamics of argon trimer by ultrashort intense laser fields. The structures of Ar_3^{3+} and Ar_3^{6+} were reconstructed. The similarity rules out the possibility that the molecular structure was changed during the multiple ionization. Thus the reconstructed structure of the argon trimer ions can represent the structure of the neutral one before the laser irradiation. In the theory, we calculated the structure of argon trimer using *ab initio* methods and compared with the reconstructed structure. The detailed discussion was included for discrepancy between the reconstructed structure and the theoretical prediction.

II. EXPERIMENT

The experiment was carried out using the combination of an intense femtosecond laser amplifier and a reaction microscope.³¹⁻³³ The argon trimer was generated by the supersonic expansion of argon gas through a 30- μm nozzle with a driving pressure of 8 bars. The laser pulse has a pulse duration of 25 fs and a central wavelength of 780 nm. The ions produced in the laser-molecule interaction were collected by a time and position-sensitive detector (RoentDek, Germany). By measuring the time of flight and the position in the detector, the ion can be identified and the initial three-dimensional momentum can be calculated. The temperature of the supersonic molecular beam, an important parameter for determining the structure distribution of argon trimer, was derived by measuring the velocity distribution of the supersonic beam. Because the momentum that the atom gained in the direction perpendicular to the laser polarization is small during the process of tunneling ionization, the velocity distribution of Ar^+ can represent that of argon atoms in the propagation direction of the supersonic beam. Figure 1 shows the velocity distribution of Ar^+ along the propagation direction of the supersonic beam and the black circles represent the experimental data. Ar^+ was generated through single ionization of argon atoms by 780-nm, 25-fs laser pulses at

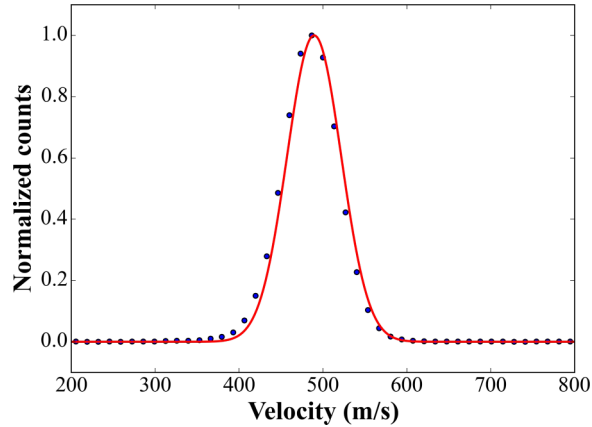


FIG. 1. Velocity distribution of argon gas along the propagation direction of the supersonic beam. The black circles represent the experimental data and the red line represents the one-peak Gaussian fitting line. The temperature of the supersonic beam was thus determined to be 6 K.

an intensity of 1.5×10^{14} W/cm². The laser polarization was perpendicular to the molecular beam direction. The temperature of the supersonic beam was determined to be 6 K by fitting the velocity distribution (full widths at half maximum), which is represented by the red line.

There are many reaction channels when the laser intensity reaches 1.3×10^{15} W/cm². One of the advantages of the reaction microscope is that the data of all reaction channels can be recorded in one experiment. In the off-line analysis, these reaction channels can be distinguished by designing some constraints to filter the experimental data. Multiple ionization followed by fragmentation of argon trimer is only a tiny fraction among all the recorded ionization events. Through carefully designing some constraints to filter the experimental data, the following three-body fragmentation channels were selected out for further analysis.

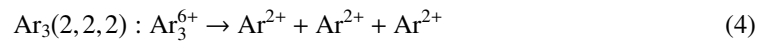
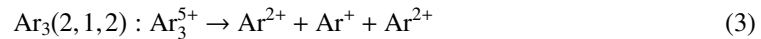
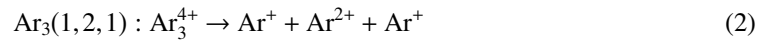


Figure 2 shows two-dimensional momentum distributions ($P_{//}$ and P_{\perp}) in the center-of-mass coordinate frame for argon atomic ions generated in the three-body fragmentation of argon trimer ions with varied charge states. The $P_{//}$ and P_{\perp} represent the momentum vectors parallel and perpendicular to the laser polarization axis, respectively. All the analysis and conclusion were based on these raw experimental data. It can be seen that there were two ring-like structures for the channels of $\text{Ar}_3(1, 2, 1)$ and $\text{Ar}_3(2, 1, 2)$ and one ring-like structure for the channels of $\text{Ar}_3(1, 1, 1)$ and $\text{Ar}_3(2, 2, 2)$. The ring-like structure indicates that argon atomic ions have almost the same kinetic energy when they carry the same charge in the three-body fragmentation process.

III. RESULTS AND DISCUSSION

Three-body fragmentation can take place through the Coulomb explosion process or the sequential fragmentation process. In the case of Coulomb explosion process, all chemical bonds break simultaneously and the three ions are generated at the same time. In the case of sequential process, the ions were generated one after the other with a time interval of the molecular rotational period of the intermediate. Due to the rotation of the intermediate, the symmetry in the geometric space will be destroyed in the momentum space. As a result, the molecular structure can be deduced only from momentum vectors of correlated atomic ions that are generated in the Coulomb explosion

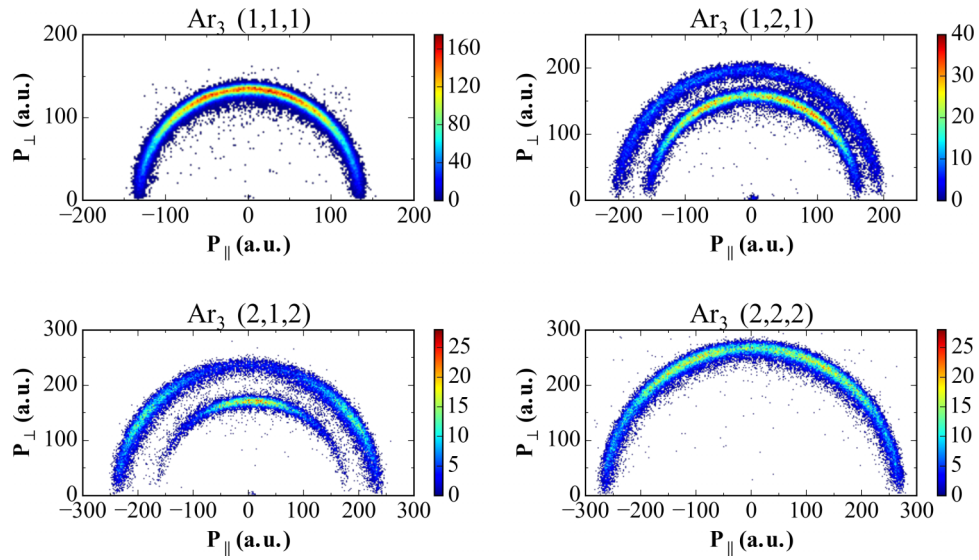


FIG. 2. Experimentally measured two-dimensional momentum distributions of correlated atomic ions generated in the three-body fragmentation of argon trimer by intense laser pulses. The laser has a central wavelength of 780 nm, a pulse duration of 25 fs and an intensity of 1.3×10^{15} W/cm².

process. Newton diagram is effective to identify the mechanism of three-body fragmentation process due to the ability of visualizing the momentum correlation of reaction products. Therefore, we display the experimental data in Newton diagrams, as shown in Figure 3. The momentum vector of an argon atomic ion is represented by an arrow fixed at one arbitrary unit. The momentum vectors

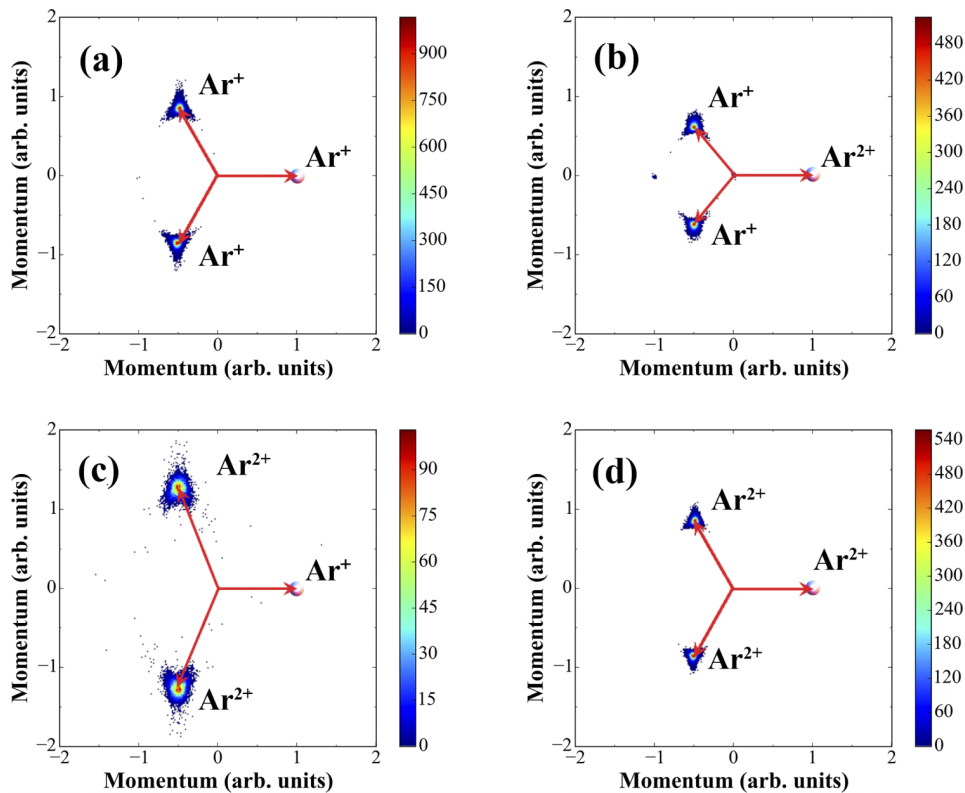


FIG. 3. Newton diagram of three-body fragmentation process of argon trimers irradiated by intense laser pulses. The laser has a central wavelength of 780 nm, a pulse duration of 25 fs and an intensity of 1.3×10^{15} W/cm².

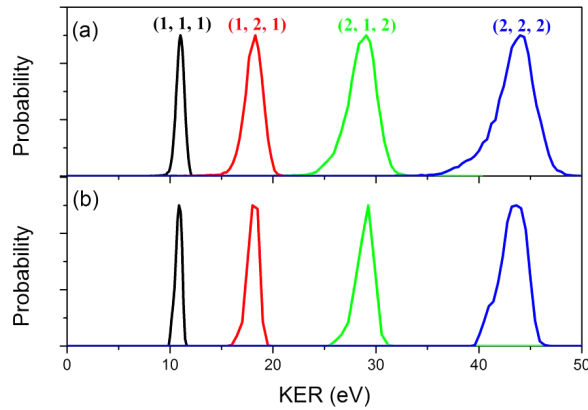


FIG. 4. (a) KER distributions for the Coulomb explosion channels Ar_3 (1, 1, 1), Ar_3 (1, 2, 1), Ar_3 (2, 1, 2) and Ar_3 (2, 2, 2). (a) experimental data, (b) theoretical calculation.

of the other two argon atomic ions are normalized to the amplitude of the first argon ion momentum vector and mapped in the left of the plot. The angle is kept unchanged between momentum vectors of any two argon ions. Because of the rotation of the intermediate, a circle structure will be exhibited in the Newton diagram if the sequential three-body fragmentation occurs.²² The lack of circle structure demonstrates that the three-body fragmentation occurs through Coulomb explosion process. Thus, the molecular structure can be deduced from momentum vectors of correlated atomic ions.

Figure 4 shows the kinetic energy release (KER) distribution, which can be obtained through the equation of $\text{KER} = \frac{1}{2m} \sum |P|^2$ with P and m being the momentum and the mass of the atomic ions generated in channels (1-4). The distributions can be well simulated by a Gaussian function with one peak for all channels. The single-peak distribution indicates that there is one isomer in the supersonic beam. The observation is consistent with our theoretical prediction that there is only one isomer for argon trimer at 6 K, the temperature of our molecular beam. The peaks locate at 11.3 eV, 18.7 eV, 29.8 eV and 44.7 eV for the channels of Ar_3 (1, 1, 1), Ar_3 (1, 2, 1), Ar_3 (2, 1, 2) and Ar_3 (2, 2, 2), respectively. One might expect the structure might be modified during the multiple ionization because the laser pulse duration is 25 fs.²⁹ Thus, the reconstructed structural parameters for ions cannot represent the structure of the neutral one before the laser irradiation. Here, using the geometric structure of Ar_3 predicted by the theory, we simulate the explosion dynamics of Ar_3 after multiple ionization based on Coulomb potential approximation. The theoretical calculated KERs are also included in Figure 4 and agree with the experimental data well for all explosion channels, especially the peak location. The agreement indicates that the nuclear motion can be neglected during the multiple ionization and the reconstructed structural parameters for ions can represent the structure of Ar_3 before the laser irradiation.

The symmetry in the geometric space can be preserved in the momentum space if the identical components carry the same charge in the three-body Coulomb explosion process.²⁵ Therefore we reconstruct the structure of Ar_3^{3+} and Ar_3^{6+} based on the momentum vectors of the atomic ions produced in the explosion channels of Ar_3 (1, 1, 1) and Ar_3 (2, 2, 2), respectively. In the process of reconstruction, Ar_3^{3+} and Ar_3^{6+} were initially given a specific geometry. Then we simulate the explosion dynamics of Ar_3^{3+} and Ar_3^{6+} with the Coulomb potential approximation. By solving the equation of nuclear motion numerically, we obtained the momentum vectors of the three argon atomic ions generated in the explosion channels of Ar_3 (1, 1, 1) and Ar_3 (2, 2, 2). The calculated momentum vectors were compared with the measured momentum vectors. The initial structure was iteratively modified until the agreement was achieved between the theory and the experiment. The structure of the argon trimer ion was thus reconstructed for each three-body explosion event. Because the molecular structure is kept unchanged during the multiple ionization, the reconstructed structural parameters of Ar_3^{3+} and Ar_3^{6+} represent those of Ar_3 before the laser irradiation. By imaging a single molecule frame by frame, we found that both the bond length and the bond angle

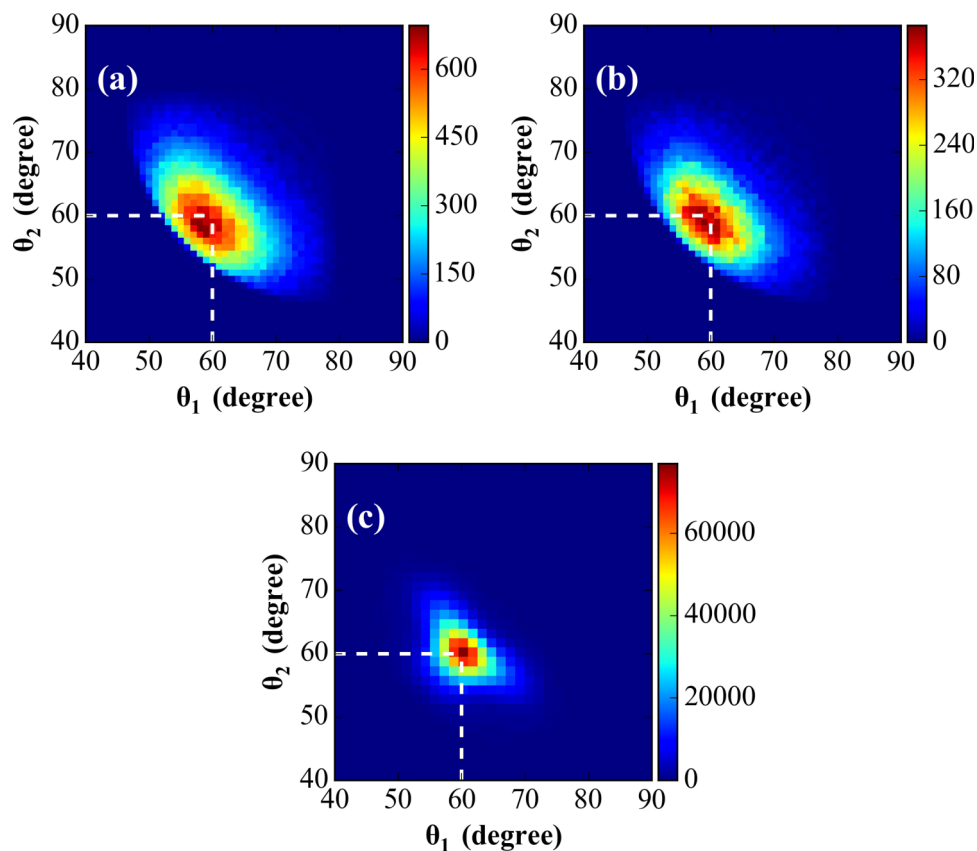


FIG. 5. Bond angle - bond angle distribution for (a) Ar_3^{3+} , (b) Ar_3^{6+} and (c) Ar_3 . Ar_3^{3+} and Ar_3^{6+} are experimentally reconstructed from the explosion channels $\text{Ar}_3(1, 1, 1)$ and $\text{Ar}_3(2, 2, 2)$, and Ar_3 is predicted by the theoretical calculation.

have a variation. Through the statistical analysis of thousands of single-molecule images, we obtain the geometric structure distribution as a function of structural parameters.

The geometrical structure distribution of argon trimer can be described by bond angle - bond angle distribution and average bond length distribution. The bond angle - bond angle distribution gives the probability to find the trimer with particular shapes. Figure 5(a) and 5(b) show the angle - angle distribution of Ar_3^{3+} and Ar_3^{6+} , reconstructed from $\text{Ar}_3(1, 1, 1)$ and $\text{Ar}_3(2, 2, 2)$ channels, respectively. It can be seen that similar structure distributions are reconstructed, both centered at $\theta_1 = \theta_2 = 60^\circ$ regardless of the explosion channels. The observation demonstrated that argon trimer fluctuates around the equilateral triangle structure. Figure 6 shows the average bond length distribution of Ar_3^{3+} and Ar_3^{6+} , reconstructed from $\text{Ar}_3(1, 1, 1)$ and $\text{Ar}_3(2, 2, 2)$ channels, respectively. Both the distribution can be fitted by a Gaussian function with one peak at 3.9 \AA . The reconstructed structural parameters, both the bond angle and the bond length, are similar for Ar_3^{3+} and Ar_3^{6+} . The similarity indicates the derived structural parameters don't depend on the channel from which the molecular structure is reconstructed. These observations further support the conclusion that the nuclear motion is frozen during the multiple ionization and the reconstructed structural parameters for ions represent the structure of Ar_3 before the laser irradiation.²⁵

In order to test the reliability of our reconstructed molecular structure, we also calculate the geometric structure of argon trimer using *ab initio* methods. The Fritz-Haber Institute *ab initio* molecular simulations (FHI-aims) package is chosen for the geometry optimization and the molecular dynamics simulations.^{34,35} To account for the weak Van der Waals interaction between the Ar atoms, the Tkatchenko-Scheffler vdW-TS method is employed in the descriptions of the inter-atomic potentials.³⁶ The molecular dynamics simulations are run in the constant-volume, constant temperature (NVT) canonical ensemble with the Andersen thermostat for the controlling of

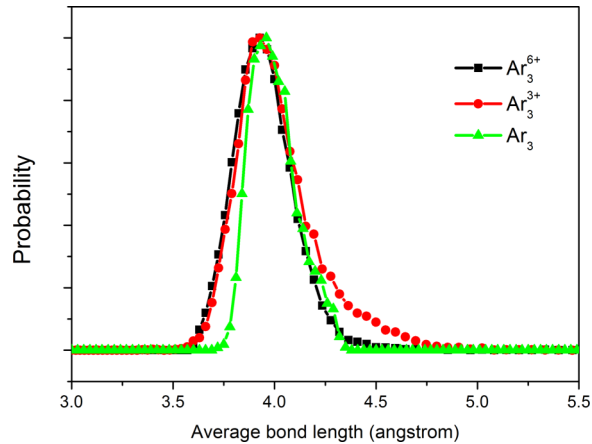


FIG. 6. Normalized average bond length distribution for Ar_3^{3+} , Ar_3^{6+} and Ar_3 . Ar_3^{3+} and Ar_3^{6+} are experimentally reconstructed from the explosion channels $\text{Ar}_3(1, 1, 1)$ and $\text{Ar}_3(2, 2, 2)$, and Ar_3 is predicted by the theoretical calculation.

the temperatures. A time step of 0.5 fs is used and a trajectory of 200 ps after thermalization is employed for the statistics of the geometric properties. The results are also included in Figures 5 and 6. It can be seen that the preferred structure also exhibits equilateral triangle with bond length peak at 3.9 Å, in agreement with the experimental results. However, a closer inspection also indicates there are some discrepancies. The main discrepancy is that the predicted structure distributions are narrower than the ones extracted from experiments, which can be attributed to two effects. One is the assumptions introduced in the process of structure reconstruction. We assumed that the momentum of each nucleus is zero before explosion and the measured momentum completely originates from the Coulomb energies during the process of structure reconstruction. In fact the momentum of argon ions will not be zero because the energy exchange between the argon ion and the ionized electron during the process of ionization.³⁷ Neglecting the initial momentum of the argon ions before explosion will overestimate the broadness of the structure distribution. The other is the presence of nuclear quantum effects at low temperatures, which we haven't taken into account in our theoretical simulations. It is known that the nuclei are intrinsically quantum particles. In standard *ab initio* molecular dynamics simulations as reported, they are treated as classical point-like particles. The presence of these nuclear quantum effects becomes more important at low temperature. And it has been shown in Ref. 17 that inclusion of such effects induces a broader distribution of such functions

IV. CONCLUSION

In summary, we have experimentally studied multiple ionization and fragmentation dynamics of argon trimer by intense femtosecond laser fields. Newton diagram demonstrated that three-body fragmentation occurs through Coulomb explosion process for argon trimer ions at different charge states. Their geometric structures were reconstructed through the momentum vectors of atomic ions generated in the Coulomb explosion process. The reconstructed structures are shown to be identical regardless of the charge state of argon trimer ions, indicating that the nuclear motion is frozen during the multiple ionization. Therefore the reconstructed structure of the argon trimer ions can represent the structure of the neutral one before the laser irradiation. This conclusion was supported further by our high level *ab initio* calculation. Very recently, the geometric structure of helium trimer was successfully determined by Coulomb explosion technique.³⁸ All these studies demonstrated Coulomb explosion technique can image the structure of clusters, particularly for floppy clusters whose structures remain difficult to be determined by available experimental techniques. The measured structural parameters can be applied to test theoretical predictions and guide the development of theoretical methods.

ACKNOWLEDGMENTS

This work was supported by the National Basic Research Program of China (No. 2013CB922403) and the National Natural Science Foundation of China (Nos. 61178019, 11474009, 11434002, and 11275008).

- ¹ R. S. Berry, *Chem. Rev.* **93**, 2379 (1993).
- ² D. J. Wales, *Science* **271**, 925 (1996).
- ³ J. Wörmer, M. Joppien, G. Zimmerer, and T. Möller, *Phys. Rev. Lett.* **67**, 2053 (1991).
- ⁴ M. Joppien, R. Karnbach, and T. Möller, *Phys. Rev. Lett.* **71**, 2654 (1993).
- ⁵ T. González-Lezana, J. Rubayo-Soneira, S. Miret-Artés, F. A. Gianturco, G. Delgado-Barrio, and P. Villarreal, *Phys. Rev. Lett.* **82**, 1648 (1999).
- ⁶ F. Luo, G. C. McBane, G. Kim, C. F. Giese, and W. R. Gentry, *J. Chem. Phys.* **98**, 3564 (1993).
- ⁷ W. Schöllkopf and J. P. Toennies, *Science* **266**, 1345 (1994).
- ⁸ R. E. Grisenti, W. Schöllkopf, J. P. Toennies, G. C. Hegerfeldt, T. Köhler, and M. Stoll, *Phys. Rev. Lett.* **85**, 2284 (2000).
- ⁹ T. Havermeier, T. Jahnke, K. Kreidi, R. Wallauer, S. Voss, M. Schöffler, S. Schöffler, L. Foucar, N. Neumann, J. Titze, H. Sann, M. Kühnel, J. Voigtsberger, J. H. Morilla, W. Schöllkopf, H. Schmidt-Böcking, R. E. Grisenti, and R. Dörner, *Phys. Rev. Lett.* **104**, 133401 (2010).
- ¹⁰ N. Sisourat, N. V. Kryzhevoi, P. Kolorenč, S. Scheit, T. Jahnke, and L. S. Cederbaum, *Nat. Phys.* **6**, 508 (2010).
- ¹¹ M. Lewerenz, *J. Chem. Phys.* **106**, 4596 (1997).
- ¹² E. Nielsen, D. V. Fedorov, and A. S. Jensen, *J. Phys. B: At. Mol. Opt. Phys.* **31**, 4085 (1998).
- ¹³ T. Gonzalez-Lezana, J. Rubayo-Soneira, S. Miret-Artés, F. A. Gianturco, G. Delgado-Barrio, and P. Villarreal, *J. Chem. Phys.* **110**, 9000 (1999).
- ¹⁴ P. Barletta and A. Kievsky, *Phys. Rev. A* **64**, 042514 (2001).
- ¹⁵ D. Bressanini and G. Morosi, *J. Phys. Chem. A* **115**, 10880 (2011).
- ¹⁶ I. Baccarelli, F. A. Gianturco, T. González-Lezana, G. Delgado-Barrio, S. Miret-Artés, and P. Villarreal, *J. Chem. Phys.* **122**, 144319 (2005).
- ¹⁷ R. Pérez de Tudela, M. Márquez-Mijares, T. González-Lezana, O. Roncero, S. Miret-Artés, G. Delgado-Barrio, and P. Villarreal, *J. Chem. Phys.* **132**, 244303 (2010).
- ¹⁸ F. Calvo, F. X. Gadéa, A. Lombardi, and V. Aquilanti, *J. Chem. Phys.* **125**, 114307 (2006).
- ¹⁹ A. Hishikawa, A. Iwamae, and K. Yamanouchi, *Phys. Rev. Lett.* **83**, 1127 (1999).
- ²⁰ F. Légaré, K. F. Lee, I. V. Litvinyuk, P. W. Dooley, A. D. Bandrauk, D. M. Villeneuve, and P. B. Corkum, *Phys. Rev. A* **72**, 052717 (2005).
- ²¹ M. Pitzer, M. Kunitski, A. S. Johnson, T. Jahnke, H. Sann, F. Sturm, L. Ph. H. Schmidt, H. Schmidt-Böcking, R. Dörner, J. Stohner, J. Kiedrowski, M. Reggelin, S. Marquardt, A. Schießer, R. Berger, and M. S. Schöffler, *Science* **341**, 1096 (2013).
- ²² C. Wu, C. Wu, D. Song, H. Su, Y. Yang, Z. Wu, X. Liu, H. Liu, M. Li, Y. Deng, Y. Liu, L.-Y. Peng, H. Jiang, and Q. Gong, *Phys. Rev. Lett.* **110**, 103601 (2013).
- ²³ B. Ulrich, A. Vredenburg, A. Malakzadeh, L. Ph. H. Schmidt, T. Havermeier, M. Meckel, K. Cole, M. Smolarski, Z. Chang, T. Jahnke, and R. Dörner, *J. Phys. Chem. A* **115**, 6936 (2011).
- ²⁴ H. Ibrahim, B. Wales, S. Beaulieu, B. E. Schmidt, N. Thiré, E. P. Fowe, É. Bisson, C. T. Hebeisen, V. Wanie, M. Giguère, J.-C. Kieffer, M. Spanner, A. D. Bandrauk, J. Sanderson, M. S. Schuurman, and F. Légaré, *Nat. Commun.* **5**, 4422 (2014).
- ²⁵ C. Wu, C. Wu, D. Song, H. Su, X. Xie, M. Li, Y. Deng, Y. Liu, and Q. Gong, *J. Chem. Phys.* **140**, 141101 (2014).
- ²⁶ X. Xie, C. Wu, Y. Liu, W. Huang, Y. Deng, Y. Liu, Q. Gong, and C. Wu, *Phys. Rev. A* **90**, 033411 (2014).
- ²⁷ K. Yamanouchi, *Science* **295**, 1659 (2002).
- ²⁸ N. Neumann, D. Hant, L. P. H. Schmidt, J. Titze, T. Jahnke, A. Czasch, M. S. Schöffler, K. Kreidi, O. Jagutzki, H. Schmidt-Böcking, and R. Dörner, *Phys. Rev. Lett.* **104**, 103201 (2010).
- ²⁹ I. Bocharova, R. Karimi, E. F. Penka, J. Brichta, P. Lassonde, X. Fu, J. Kieffer, A. D. Bandrauk, I. Litvinyuk, J. Sanderson, and F. Légaré, *Phys. Rev. Lett.* **107**, 063201 (2011).
- ³⁰ C. Wu, Y. Yang, Z. Wu, B. Chen, H. Dong, X. Liu, Y. Deng, H. Liu, Y. Liu, and Q. Gong, *Phys. Chem. Chem. Phys.* **13**, 18398 (2011).
- ³¹ R. Dörner, V. Mergel, O. Jagutzki, L. Spielberger, J. Ullrich, R. Moshhammer, and H. Schmidt-Böcking, *Phys. Rep.* **330**, 95 (2000).
- ³² J. Ullrich, R. Moshhammer, A. Dorn, R. Dörner, L. Ph. H. Schmidt, and H. Schmidt-Böcking, *Rep. Prog. Phys.* **66**, 1463 (2003).
- ³³ C. Wu, C. Wu, Y. Yang, Z. Wu, X. Liu, X. Xie, H. Liu, Y. Deng, Y. Liu, H. Jiang, and Q. Gong, *J. Mod. Opt.* **60**, 1388 (2013).
- ³⁴ V. Blum, R. Gehrke, F. Hanke, P. Havu, V. Havu, X. G. Ren, K. Reuter, and M. Scheffler, *Comput. Phys. Commun.* **180**, 2175 (2009).
- ³⁵ <https://aimsclub.fhi-berlin.mpg.de/>.
- ³⁶ A. Tkatchenko and M. Scheffler, *Phys. Rev. Lett.* **102**, 073005 (2009).
- ³⁷ X. Xie, C. Wu, Z. Yuan, D. Ye, P. Wang, Y. Deng, L. Fu, J. Liu, Y. Liu, and Q. Gong, *Phys. Rev. A* **92**, 023417 (2015).
- ³⁸ J. Voigtsberger, S. Zeller, J. Becht, N. Neumann, F. Sturm, H.-K. Kim, M. Waitz, F. Trinter, M. Kunitski, A. Kalinin, J. Wu, W. Schöllkopf, D. Bressanini, A. Czasch, J. B. Williams, K. Ullmann-Pfleger, L. Ph. H. Schmidt, M. S. Schöffler, R. E. Grisenti, T. Jahnke, and R. Dörner, *Nat. Commun.* **5**, 5765 (2014).